This is a repository copy of *Fluorescence recovery after photobleaching to study the dynamics of membrane-bound proteins in vivo using the Drosophila embryo*.

Article:

Fluorescence Recovery After Photobleaching to study the dynamics of membrane bound proteins *in vivo* using the *Drosophila* embryo

Joshua Greig[1], Natalia A. Bulgakova[1, *]

[1] Department of Biomedical Science and Bateson Centre, The University of Sheffield, Sheffield S10 2TN, United Kingdom.

[*] Corresponding author: n.bulgakova@sheffield.ac.uk

Keywords:

protein dynamics, membrane proteins, E-cadherin, cell-cell adhesion, FRAP, diffusion, endocytosis

Running header: FRAP to study the dynamics of proteins *in vivo*

Abstract

The epithelial-to-mesenchymal transition is a highly dynamic cell process and tools such as Fluorescence recovery after photobleaching (FRAP), which allow the study of rapid protein dynamics, enable the following of this process *in vivo*. This technique uses a short intense pulse of photons to disrupt the fluorescence of a tagged protein in a region of a sample. The fluorescent signal intensity after this bleaching is then recorded and the signal recovery used to provide an indicator of the dynamics of the protein of interest. This technique can be applied to any fluorescently tagged protein, but membrane-bound proteins present an interesting challenge as they are spatially confined and subject to specialized cellular trafficking. Several methods of analysis can be applied which can disentangle these various processes and enable the extraction of information from the recovery curves. Here we describe this technique when applied for the quantification of the plasma membrane-bound E-cadherin protein *in vivo* using the epidermis of the late embryo of *Drosophila melanogaster (Drosophila)* as an example of this technique.

1. Introduction

The maintenance of epithelial tissue, epithelial-to-mesenchymal transitions (EMTs), and the migration of mesenchymal cells relies on dynamic turnover of transmembrane proteins, such as cadherins and integrins [1–5]. These membrane proteins are confined in space, with diffusion along the plane of the lipid bilayer, but they can move in and out of the plasma membrane using the specialized cellular mechanism of endocytic internalization and recycling [6–9]. Alterations to this dynamic turnover, both diffusional and endocytic trafficking, result in profound changes in cell behaviour, and in some cases can induce or prevent EMT [10,11]. Therefore, the total amount of a transmembrane protein in a specimen provides only part of the information about cell-cell interactions and cellular behaviour. To fully understand these processes, one must measure the dynamics of the protein of interest *in vivo* in living cells and tissues.

Fluorescence recovery after photobleaching (FRAP) is a fluorescent microscopy technique which allows one to do precisely this and has made a significant impact on the understanding of the functions of proteins and regulation of cell adhesion and migration [12–16]. In essence, the technique relies on the disruption of the signal from a fluorescently tagged protein in a portion of a sample, this is achieved by bleaching a region with a short, intense pulse of photons. One then measures the fluorescence in the bleached area for a period following the bleaching to record the recovery of the fluorescence signal. Importantly the proteins in the bleached area are still present but are merely "dark" due to the loss of fluorescence. Therefore, what is measured is the exchange of proteins between the bleached area and the rest of the cell. Carefully designed FRAP experiments enable not only the determination of the overall dynamics of a transmembrane protein, but also allows one to distinguish the contributions of both the diffusional and endocytic trafficking processes and to determine the specific changes in each.

The performance of a FRAP experiment is reliant upon the following steps: preparation of the sample, calibration of the microscope settings, performing and acquiring the data on the microscope, analysing the data, fitting the recovery curve, and interpreting the results. Here, we use an example of FRAP performed on the membrane bound epithelial cadherin (E-cad) molecule which has been tagged

with the fluorophore EGFP [17]. The theoretical aspects of FRAP are extensively described in other publications [18–23]. We therefore focus on the practical aspects of performing FRAP, which will allow anyone with access to a confocal microscope to do the whole procedure from sample preparation to the final result.

We and other research groups have shown that the E-cad signal recovers in *Drosophila* and mammalian cells by both diffusional and endocytic recycling mechanisms, which are kinetically distinct [1,15,24,25]. Here, we specifically use the example of the epidermis of the stage 15 *Drosophila* embryo. However, aside from sample preparation, the same protocol, calibration, and analysis are applicable for other proteins and cell types. Finally, we outline the main considerations for designing and analysing FRAP experiments.

2 Materials

2.1 Flies

*ubi::*E-cad-GFP (Bloomington, 58471 or 58742) flies can be used as the source of E-cad-GFP (*see* **Note** 1). The copy number of E-cad-GFP and endogenous E-cad loci must be equal in the control and experimental animals, as diffusional coefficients calculated from recovery curves depend on the total concentration of the tagged protein [26]. Alternatively, flies with endogenously tagged *shg::*E-cad-GFP (Bloomington 60584) can be used. In our experience, ubiquitously and endogenously tagged E-cad behaves identically in FRAP experiments [27].

2.2 Reagents and equipment

1. Apple juice plates for collection of embryos: 60mm plates filled with 10 ml of apple juice agar media (for 50 plates: 15g agar, 400ml distilled water, 100ml apple juice, 7.5ml 10% nipagin in absolute ethanol) and baking yeast.

2. Collection chambers, which tightly fit the apple juice plates and allow oxygen access to the flies.

3. Embryo preparation: bleach and deionized H_2O.

4. Filtration nets: using a razor blade, cut a 15 ml Falcon tube at about 11.5 ml mark and make a hole of about 1 cm diameter in its lid. Then, cut a nylon net out of a 100 μm pore cell strainer, and assemble the embryo filtration net by inserting the net between the lid and tube.

4. Dissection needles.

5. Microscope slides.

6. Heptane glue: incubate 5 cm length of adhesive tape (Sellotape 1447052 is used due to no toxic effects) with 2 ml Heptane for at least 24 hours prior to conducting experiments in a sealed glass vial.

7. Halocarbon oil 27.

8. A confocal microscope with a 488 laser and sufficiently sensitive detectors.

9. Software packages: Fiji (https://fiji.sc), Microsoft Excel, and appropriate statistical packages, e.g. Matlab (https://www.mathworks.com/products/matlab.html), R (https://www.r-project. org), GraphPad Prism (https://www.graphpad.com/scientific-software/prism/).

3 Methods

3.1 Embryo collection

1. For synchronized egg collections, set at least 50 virgin female and 20 male flies to mate for 1 day in a collection chamber with an apple juice plate attached to the bottom of the chamber at 25°C. A measure of yeast paste should be applied to apple juice plates with a spatula before placing with the flies in the embryo collection chambers.

2. Collect embryos at 25°C for a 1.5-hour time interval, the plates used for these collections should have only a small measure of yeast and be prewarmed at 25°C before use. Allow them to develop at 18°C for 21 hours to reach the desired developmental stage, at the end of dorsal closure corresponding to late stage 15.

3. Dislodge the embryos from the surface of the apple juice agar by applying a small measure of deionized water and brushing surface with a paint brush.

4. Dechorionate the embryos by immersing in a 1:1 sodium hypochlorite (bleach) and deionized water solution for 5 minutes followed by filtration through an in-house made embryo filtration net and extensive washing with deionized water.

3.2 Mounting of samples on microscope slides

1. Prepare the imaging microscope slide (Fig. 1a): attach two 22x22 coverslips at either end of a microscope slide using a spot of nail varnish to create a bridge, then either add a strip of adhesive tape across the central channel on the slide between the two coverslips (orthogonal to the long axis of the slide) or add a few drops of heptane glue, spread it thinly with another coverslip, and allow heptane to evaporate (Fig. 1b). Keep the slide covered with a plate to avoid dust.

2. Transfer dechorionated embryos to apple juice agar segments on a microscope slide using a paint brush (Fig. 1c-d).

3. Select the correct genotype using a fluorescent stereomicroscope and specific fluorescent markers, e.g. presence of the fluorophore of interest or specific fluorescently-tagged balancer chromosomes. For stage 15 embryos we routinely use balancers with GFP driven in the mesoderm with *twist* promoter (Bloomington 6662 and 6663) or YFP expressed in mandibular and maxillary segments with *Deformed* promoter (Bloomington 8578 and 8704). Then transfer the desired embryos to an adjacent segment of apple juice agar, while orientating them relative to one another and according to their anterior-posterior and dorso-ventral axis (*see* **Note 2**, Fig. 1e-f).

4. Transfer embryos to prepared slide (see 3.2.1) by pressing this slide delicately against the apple juice segment containing the aligned embryos (*see* **Note 3**, Fig. 1g).

5. Add 50 µl of halocarbon oil over the embryos so that embryos are fully covered (add dropwise) and leave for 10 minutes (Fig. 1h).

6. Apply a 22x40 coverslip over the embryos, it is best to gradual lower the coverslip to minimise bubble entrapment. Seal the ends of the coverslip by using nail varnish and allow to dry for few minutes before taking to the microscope, this prevents any slippage of the coverslip or wet nail varnish coming into contact with the lens of the microscope (Fig. 1i).

3.3 Determining the parameters for the FRAP experiments

1. Decide on the shape, number and size of the areas to be bleached (<u>R</u>egions <u>O</u>f <u>I</u>nterest, ROI, *see* **Note 4**). Circular areas of 0.5-1 μm diameter are applicable to most cases, and we use 2-3 circular areas of 1 μm diameter ensuring that only one event occurs for a cell and that no adjacent cells are bleached. **Important**: the same size bleach spot within a sample and between genotypes must be used during an experiment [18] (*see* **Note 5**).

2. Perform test bleaching to achieve an appropriate level of bleaching (*see* **Note 6**) within a minimal time exposure (*see* **Note 7**). Start by bleaching the selected region for 10 msec with 100% 488 nm laser. If the bleaching is too strong (*see* **Note 6**) reduce the laser intensity and bleaching time. If the fluorescence intensity in a selected ROI immediately after bleaching is above 40% of initial pre-bleach intensity, increase the bleaching time up to 20 msec or/and use 405 nm laser instead.

3. Record a freerun time-series (no time interval between frames) of the fluorescence recovery in a z-stack spanning the structure of interest, e.g. adherens junction, for 2-5 min starting by using the lowest power, which yields sufficient clearly visible signal, during this phase (we use 1% intensity of 488 nm laser). This will enable determine imaging parameters which enable recording the recovery as fast as possible (*see* **Note 8**) while minimizing any additional photobleaching (*see* **Note 9**).

4. Calculate acquisitional photobleaching by comparing the fluorescence intensity of the control (unbleached) ROI at the end of the time series to its prebleach value; and the initial recovery (between the first and second time points after bleaching, see **3.5**). Use these values to adjust the imaging parameters. If the acquisitional bleaching is more than 15%, reduce the laser power or increase the scanning speed (*see* **Note 9**). If the initial recovery is greater than 5%, reduce intervals between time points by reducing image resolution, applying digital zoom, or/and increasing scanning speed (*see* **Note 8**). If the initial recovery is below 1%, increase the interval between time points.

5. Repeat steps 3-4 until desired levels of acquisitional bleaching and initial recovery are achieved, while sufficient spatial resolution (the ROI below 10 pixel in diameter are likely to introduce large noise due to even mild movements in XY plane). For E-cad-GFP we use 6x 0.38 μm sections which span the entire depth of adherens junction. Each section is 320 x 320 pixel, with spatial resolution 0.093 μm/pixel, and are taken every 20 sec. We use a 63x magnification lens with a numerical

aperture (NA) of 1.4, 1-2% laser power, 2 μs/pixel dwell with amplification of the Hv/gain of the PMT for the optimal image acquisition.

6. Calculate the recovery at the five last time points to ensure that the duration of recording the recovery is sufficient to enable measurement and identification of several components (*see* **Note 10**). If the change in the fluorescence intensity of the ROI during these time points is greater than 1% of initial intensity, increase the time of recording. In this case, one must ensure that acquisitional photobleaching remains low. If the change determined is lower than 1%, calculate the recovery at the previous five time points. Use the last time point, at which the recovery of the final five time points remains below 1%, to determine the duration required to record the recovery.

3.4 Bleaching and acquisition

1. Select a region of the epidermis for the experiment, set up a z-stack, and select the ROI (Fig. 2a-d).

2. Set up the following experiment sequence (according to specific software and microscope): a 4D z-stack and time series at selected resolution, time interval and duration with bleaching activated just before the start of the second or third z-section.

3. For measuring the dynamics of E-cad-GFP in *Drosophila* embryos, use 8-10 embryos with 2-3 measurements per embryo. Although the recovery of individual bleach events are likely to be noisy and subjected to fluctuations in intensities, this size of the dataset enables one to obtain a good and stable averaged recovery curve (Fig. 3).

3.5 Signal intensity measurements and data processing

1. Open the raw ".oib/.czi" files and use the grouped z-projector plugin to compile each time point as an average intensity projection (*see* **Note 11**): for E-cad-GFP average intensity complied by 6 for each stack taken, yields 45 timepoints. We use Fiji (https://fiji.sc) for this purpose.

2. Select a region in the centre of a cell without bleached junctions and measure intensity using a ROI of the same size as used bleach spots across the time series (*see* **Note 12**, Fig. 2e).

3. Perform the same for a control region, which is a junction between two cells whose E-cad was not bleached, and the bleached regions (*see* **Note 13**, Fig. 2e).

4. Subtract background and normalize fluorescence intensity of the bleached region as following:

$I_n = (F_n - BG_n)/(FC_n - BG_n)$, where F_n – intensity of the bleached ROI at the time point n, FC_n –

intensity of the control unbleached ROI of the same size at the plasma membrane at the time point n,

and BG_n – background intensity, measured with the same size ROI in cytoplasm at the time point n.

5. Calculate the relative recovery at each time point using the following formula: $R_n =$

$(I_n - I_1)/(I_0 - I_1)$, where I_n, I_1 and I_0 are: the normalized intensities of bleached ROI and time point

n, immediately after photobleaching, and before photobleaching respectively (Fig. 3).

6. Perform nonlinear regression analysis to test for the best fit model using suitable statistical package,

e.g. GraphPad Prism (https://www.graphpad.com/scientific-software/prism). Fit the recovery to a

single exponential model in a form of $f(t) = 1 - F_{im} - A_1 e^{-t/T_{fast}}$, and to bi-exponential model in

a form of $f(t) = 1 - F_{im} - A_1 e^{-t/T_{fast}} - A_2 e^{-t/T_{slow}}$, where F_{im} is a size of the immobile fraction,

T_{fast} and T_{slow} are the half times, and A_1 and A_2 are amplitudes of the fast and slow components of the

recovery. Use an F-test to choose the model and compare datasets (*see* **Notes 14-15** and Fig. 3).

4 Notes

1. Several theoretical aspects should be taken into consideration when selecting the fluorophore. The

ideal fluorophore for FRAP purposes has the optical properties of being bright, yet sufficiently

photostable for the long low-level excitation required for the course of the experiment. Furthermore, it

should easily undergo a non-reversible conversion when bleached, should not affect the dynamics of

the protein to which it is tagged and importantly should not dimerize. Early variants of GFP were

susceptible to dimerization, which alters recovery kinetics [28,29], thus skewing the results. For most

purposes EGFP, Venus, or Emerald are the most suitable for FRAP (for more information on

properties of specific fluorescent proteins see [30]). However, when using EGFP or any other GFP

derivatives it is important to consider that although infrequent (less than 15% of these fluorophores)

undergo spontaneous photoswitching – reversible photobleaching with molecules regaining

fluorescence after a period of time [31]. Therefore, when using these fluorescent proteins for FRAP it

may be a necessary to apply a correction to minimize the contribution of photoswitching in the signal

recovery [32]. Finally, tagging proteins with EGFP can have an effect on its behaviour [33,34]. This can be mitigated if one is careful in the selection of the site of tagging, in particular avoiding locations which might affect protein functions or interactions. However, whenever possible we would recommend confirming that the tagged protein retains the normal behaviour and is able to substitute for the endogenous protein. Additionally, it is crucial to use the same tagged proteins in control and experimental animals or cells.

2. *Drosophila* embryos are bean-shaped with convex side corresponding to embryo ventral side and concave to its dorsal side. The anterior of the embryos is marked by presence of micropyle. Therefore, to orient embryos correctly for imaging using an upright microscope they should be aligned with dorsal side down on the segment of apple juice agar. We also recommend aligning all embryos in the same anterior-posterior orientation as this simplifies both the transfer to the slide and imaging.

3. When transferring embryos to a slide, it is important to bear in mind that the embryos are comparatively fragile. Therefore, when pressing the surface of the adhesive strip microscope slide to the embryos positioned on the apple juice segments it is recommended that a delicate amount of pressure is applied and only for a brief moment. If possible, use a dark bench to better visualise the embryos on the apple juice segments which appear similar to small rice grains to the unaided eye.

4. Circular areas of a Gaussian intensity profile provide the most straightforward system for the following analysis, although an approach for calculating diffusion coefficients when using arbitrary bleach area geometries has been proposed [35]. The size of the bleached area must be small enough so that the unbleached protein is in excess, so that the contribution of bleached protein in the exchange can be neglected. Alternatively, a whole-cell FRAP can be used to determine the rate of new protein production [36].

5. While fixing the size of a bleach spot is important during each series of experiments, due to the change in the diffusional coefficient with bleach spot size and diameter [15,23], a comparison of the recovery when applying different bleach spot sizes can be used to confirm and test the diffusional component of the recovery. This is due to the half time of the recovery being affected by the spot size in the case of recovery primarily through diffusion, but not when binding reactions predominate over diffusion [23]

6. It is important to achieve a sufficient photobleaching depth (the amount of signal lost relative to pre-bleach) for a meaningful recovery while avoiding overbleaching. If over 80% of the initial signal is bleached, a Gaussian approximation of the bleached region is no longer valid, meaning that most common mathematical models cannot be applied [22,28]. Additionally, excessive bleaching might cause photodamage due to localized heating [18,37]. One approach which one can use to test for any changes in protein dynamics due to photodamage is sequential bleaching. Namely, to bleach an area, allow it to recover, then bleach it again with the same parameters. In the absence of photodamage, the recovery of the second bleach event will have the same dynamics (number and half-times of components) but will be close to complete (proportionally to the extent of the first bleaching round) due to the immobile fraction having already been bleached in the first round. This control for photodamage has been applied by our group and others [15,38] and is an important consideration when starting a new FRAP experiment on a newly tagged protein or in a new system. In our experience, the best means of producing consistent results without photodamage is achieved when the fluorescent protein is bleached to 20-40% of the initial fluorescent intensity. For E-cad-GFP we use 8 scans with 50-70% laser power using 488 nm wavelength laser.

7. The time to achieve sufficient bleaching must be minimized for two reasons. First, one needs to consider that protein dynamics do not cease while photobleaching is being performed, which causes misinterpretation of the kinetics due to the corona effect [39]. Longer bleaching times will lead to bigger bleached areas due to the bleached protein moving out of the spot where laser is applied. Secondly, localized heating mentioned above increases with bleaching time, which could intensifying potential damage to cells and proteins [37]. Photobleaching times below 20 msec, and ideally within 6-12 msec, were suggested to be appropriate for determining diffusion coefficients of monomeric GFP [29,37], and approaches to measure actual bleached area have also been suggested [29].

8. To achieve sufficient temporal resolution during the acquisition of fluorescence recovery, it is necessary to record the recovery at intervals which are smaller than the half time of the fastest recovery component. Although as fast an acquisition as 1/10 of the half time is recommended in some publications [28], in our experience, for recording E-cad-GFP, 20 sec intervals are sufficient to detect

a diffusional component with the half time about 25 sec. For calibration, the aim is to achieve sufficient temporal resolution while maintaining maximal possible spatial resolution.

9. The photobleaching during the acquisition of the fluorescence recovery should be minimized as much as possible to obtain the most accurate information about the dynamics [40]: deviation by more than 10-15% is usually suggestive of excessive acquisitional bleaching [28].

10. It has been suggested that the duration of recovery acquisition should be 7-10 times longer than the characteristic half time of the slowest detected component [28]. In our experience, 3 times longer acquisition is sufficient for a reliable estimation of both half times and maximum recovery [15]. Furthermore, theoretically the signal ought to completely recover with a given time. For E-cad in the *Drosophila* this has been calculated to be a period of two hours, through recovery of the "immobile" fraction by slow E-cad degradation and the addition of newly synthesized protein [41].

11. We use average intensity projections instead of maximum projections, as it considers not only protein concentration (intensity), but also distribution along the z-axis, i.e. junction width, and is reflective of the total protein amount. For example, a junction with the same E-cad density, but shorter in the z-axis will result in the same intensity when maximum projection is used as control and might skew interpretation of the results.

12. There are several plugins which allow one to perform registration of a time series, i.e. compensation for tissue movement over time, such as "Register Virtual Stack Slices" in ImageJ. However, even when using such scripts, we recommend manually tracking or checking to control for ROI position when measuring intensities. For example, changes in the membrane curvature is observed in epithelial cells, which might shift the ROI position even if the cell position is correctly registered.

13. The best are control regions which are located in as close z position to the beached region as possible and have a relatively similar intensity, as the side-effects of image acquisition such as z-drift and photobleaching will be comparable, enabling more accurate normalization. Therefore, while one control region might be possible to use for all bleached ROIs, it might be advisable to select a different appropriate control region for each bleached ROI in a time series.

14. Although more accurate equations exist for the various hypothetical methods of how protein exchanges and the signal recovers, e.g. diffusion only , diffusion-coupled, diffusion-uncoupled, [23] we find that a general fit by using a sum of exponential components provides a valid linearization of a set of nonlinear first-order differential equations according Lyapunov's first method [42,43].

15. If the recovery is fit by a single exponential model, and appropriate tests are performed to determine whether the recovery occurs via diffusion or reaction-dominant mechanisms, it is possible to obtain additional information about protein dynamics. In the case of a pure-diffusion dominant recovery, the exact solution exists for a circular bleach area in form: $f(t) = e^{-T_D/2t}(I_0\left(T_D/2t\right) + I_1\left(T_D/2t\right))$, where I_0 and I_1 are modified Bessel functions of the first kind. In this case, $T_D = w^2/D_f$, where w is the radius of the circular beam, and D_f is the diffusion coefficient [20,21]. If the recovery is reaction dominant, the following solution describes the recovery: $f(t) = 1 - C_{eq}e^{-k_{off}t}$, where C_{eq} is a constant which depends only on the dissociation (off-rate, k_{off}) and association (pseudo-on-rate, k_{on}) of the reaction [20,44]. We would like to highlight that in this case the rate of the reaction depends only on the off-rate and does not reflect the on-rate, which can be a common misapprehension when interpreting the results of FRAP experiments [4].

References

1. Erami Z, Timpson P, Yao W, Zaidel-Bar R, Anderson KI (2015) There are four dynamically and functionally distinct populations of E-cadherin in cell junctions. *Biol Open* bio.014159.

2. Foote HP, Sumigray KD, Lechler T (2013) FRAP Analysis Reveals Stabilization of Adhesion Structures in the Epidermis Compared to Cultured Keratinocytes. *PLOS ONE* **8**: e71491.

3. Indra I, Choi J, Chen C-S, Troyanovsky RB, Shapiro L, Honig B, Troyanovsky SM (2018) Spatial and temporal organization of cadherin in punctate adherens junctions. *Proc Natl Acad Sci* 201720826.

4.   Wehrle-Haller B (2007) Analysis of Integrin Dynamics by Fluorescence Recovery After Photobleaching. In Coutts AS (ed.), *Adhesion Protein Protocols* pp 173–201. Humana Press, Totowa, NJ.

5.   Cluzel C, Saltel F, Lussi J, Paulhe F, Imhof BA, Wehrle-Haller B (2005) The mechanisms and dynamics of αvβ3 integrin clustering in living cells. *J Cell Biol* **171**: 383–392.

6.   Changede R, Sheetz M (2017) Integrin and cadherin clusters: A robust way to organize adhesions for cell mechanics. *BioEssays* **39**: e201600123.

7.   Nanes BA, Kowalczyk AP (2012) Adherens junction turnover: regulating adhesion through cadherin endocytosis, degradation, and recycling. *Subcell Biochem* **60**: 197–222.

8.   Woichansky I, Beretta CA, Berns N, Riechmann V (2016) Three mechanisms control E-cadherin localization to the zonula adherens. *Nat Commun* **7**: 10834.

9.   Nader GPF, Ezratty EJ, Gundersen GG (2016) FAK, talin and PIPKIγ regulate endocytosed integrin activation to polarize focal adhesion assembly. *Nat Cell Biol* **18**: 491–503.

10.   Lu Z, Ghosh S, Wang Z, Hunter T (2003) Downregulation of caveolin-1 function by EGF leads to the loss of E-cadherin, increased transcriptional activity of beta-catenin, and enhanced tumor cell invasion. *Cancer Cell* **4**: 499–515.

11.   Wheelock MJ, Shintani Y, Maeda M, Fukumoto Y, Johnson KR (2008) Cadherin switching. *J Cell Sci* **121**: 727–735.

12.   Pasapera AM, Schneider IC, Rericha E, Schlaepfer DD, Waterman CM (2010) Myosin II activity regulates vinculin recruitment to focal adhesions through FAK-mediated paxillin phosphorylation. *J Cell Biol* **188**: 877–890.

13.   Stutchbury B, Atherton P, Tsang R, Wang D-Y, Ballestrem C (2017) Distinct focal adhesion protein modules control different aspects of mechanotransduction. *J Cell Sci* **130**: 1612–1624.

14.   Nanes BA, Chiasson-MacKenzie C, Lowery AM, Ishiyama N, Faundez V, Ikura M, Vincent PA, Kowalczyk AP (2012) p120-catenin binding masks an endocytic signal conserved in classical cadherins. *J Cell Biol* **199**: 365–380.

15. Bulgakova NA, Grigoriev I, Yap AS, Akhmanova A, Brown NH (2013) Dynamic microtubules produce an asymmetric E-cadherin–Bazooka complex to maintain segment boundaries. *J Cell Biol* **201**: 887–901.

16. Ratheesh A, Gomez GA, Priya R, Verma S, Kovacs EM, Jiang K, Brown NH, Akhmanova A, Stehbens SJ, Yap AS (2012) Centralspindlin and α-catenin regulate Rho signalling at the epithelial zonula adherens. *Nat Cell Biol* **14**: 818–828.

17. Oda H, Tsukita S (2001) Real-time imaging of cell-cell adherens junctions reveals that Drosophila mesoderm invagination begins with two phases of apical constriction of cells. *J Cell Sci* **114**: 493–501.

18. De Los Santos C, Chang C-W, Mycek M-A, Cardullo RA (2015) FRAP, FLIM, and FRET: Detection and analysis of cellular dynamics on a molecular scale using fluorescence microscopy. *Mol Reprod Dev* **82**: 587–604.

19. Day CA, Kraft LJ, Kang M, Kenworthy AK (2012) Analysis of protein and lipid dynamics using confocal fluorescence recovery after photobleaching (FRAP). *Curr Protoc Cytom Editor Board J Paul Robinson Manag Ed Al* **CHAPTER**: Unit2.19.

20. Sprague BL, Pego RL, Stavreva DA, McNally JG (2004) Analysis of Binding Reactions by Fluorescence Recovery after Photobleaching. *Biophys J* **86**: 3473–3495.

21. Soumpasis DM (1983) Theoretical analysis of fluorescence photobleaching recovery experiments. *Biophys J* **41**: 95–97.

22. Axelrod D, Koppel DE, Schlessinger J, Elson E, Webb WW (1976) Mobility measurement by analysis of fluorescence photobleaching recovery kinetics. *Biophys J* **16**: 1055–1069.

23. Sprague BL, McNally JG (2005) FRAP analysis of binding: proper and fitting. *Trends Cell Biol* **15**: 84–91.

24. Bulgakova NA, Brown NH (2016) Drosophila p120-catenin is crucial for endocytosis of the dynamic E-cadherin-Bazooka complex. *J Cell Sci* **129**: 477–482.

25. de Beco S, Gueudry C, Amblard F, Coscoy S (2009) Endocytosis is required for E-cadherin redistribution at mature adherens junctions. *Proc Natl Acad Sci U S A* **106**: 7010–7015.

26. Safranyos RG, Caveney S, Miller JG, Petersen NO (1987) Relative roles of gap junction channels and cytoplasm in cell-to-cell diffusion of fluorescent tracers. *Proc Natl Acad Sci U S A* **84**: 2272–2276.

27. Greig J, Bulgakova NA (2018) E-cadherin endocytosis is modulated by p120-catenin through the opposing actions of RhoA and Arf1. *bioRxiv* 477760.

28. Klein C, Waharte F (2010) Analysis of Molecular Mobility by Fluorescence Recovery After Photobleaching in Living Cells. 12.

29. Kitamura A, Kinjo M (2018) Determination of diffusion coefficients in live cells using fluorescence recovery after photobleaching with wide-field fluorescence microscopy. *Biophys Physicobiology* **15**: 1–7.

30. Kremers G-J, Gilbert SG, Cranfill PJ, Davidson MW, Piston DW (2011) Fluorescent proteins at a glance. *J Cell Sci* **124**: 157–160.

31. Sinnecker D, Voigt P, Hellwig N, Schaefer M (2005) Reversible photobleaching of enhanced green fluorescent proteins. *Biochemistry* **44**: 7085–7094.

32. Mueller F, Morisaki T, Mazza D, McNally JG (2012) Minimizing the impact of photoswitching of fluorescent proteins on FRAP analysis. *Biophys J* **102**: 1656–1665.

33. Jian X, Cavenagh M, Gruschus JM, Randazzo PA, Kahn RA (2010) Modifications to the C-terminus of Arf1 alter cell functions and protein interactions. *Traffic Cph Den* **11**: 732–742.

34. Hoffmann A, Dannhauser PN, Groos S, Hinrichsen L, Curth U, Ungewickell EJ (2010) A comparison of GFP-tagged clathrin light chains with fluorochromated light chains in vivo and in vitro. *Traffic Cph Den* **11**: 1129–1140.

35. Blumenthal D, Goldstien L, Edidin M, Gheber LA (2015) Universal Approach to FRAP Analysis of Arbitrary Bleaching Patterns. *Sci Rep* **5**: 11655.

36. Huang J, Huang L, Chen Y-J, Austin E, Devor CE, Roegiers F, Hong Y (2011) Differential regulation of adherens junction dynamics during apical–basal polarization. *J Cell Sci* **124**: 4001–4013.

37. Axelrod D (1977) Cell surface heating during fluorescence photobleaching recovery experiments. *Biophys J* **18**: 129–131.

38. Lalo U, Allsopp RC, Mahaut-Smith MP, Evans RJ (2010) P2X1 receptor mobility and trafficking; regulation by receptor insertion and activation. *J Neurochem* **113**: 1177–1187.

39. Weiss M (2004) Challenges and artifacts in quantitative photobleaching experiments. *Traffic Cph Den* **5**: 662–671.

40. Wu J, Shekhar N, Lele PP, Lele TP (2012) FRAP Analysis: Accounting for Bleaching during Image Capture. *PLoS ONE* **7**:.

41. Iyer KV, Piscitello-Gómez R, Paijmans J, Jülicher F, Eaton S (2019) Epithelial Viscoelasticity Is Regulated by Mechanosensitive E-cadherin Turnover. *Curr Biol* **29**: 578-591.e5.

42. Parks PC (1992) A. M. Lyapunov's stability theory—100 years on. *IMA J Math Control Inf* **9**: 275–303.

43. LYAPUNOV AM (1992) The general problem of the stability of motion. *Int J Control* **55**: 531–534.

44. Bulinski JC, Odde DJ, Howell BJ, Salmon TD, Waterman-Storer CM (2001) Rapid dynamics of the microtubule binding of ensconsin in vivo. *J Cell Sci* **114**: 3885–3897.

Figure 1. Preparation of the embryo samples for live imaging. (**a-i**) The complete steps of the process of preparing the microscope slides. (**a**) Bridge created by affixing two 22x22 coverslips by a droplet of nail varnish at either edge of the microscope slide (slide further away is before coverslips added). (**b**) On the slide with the bridge, a strip of scotch tape is placed between coverslips occupying the canal area (arrowheads show direction). (**c**) Two segments of apple juice agar are placed on a separate microscope slide. (**d**) After dechorionation the embryos are transferred onto one of the apple juice segments by using a paint brush. (**e**) Use a needle or forceps to transfer the desired embryos to the adjacent apple juice segment and align them in correct orientation. (**f**) Positioning of the embryos on the apple juice segments. The embryos are orientated with anterior left. Most are orientated with ventral side up, the bottom is position laterally to show the bean shape and curvature which can aid in distinguishing the dorsal and ventral. The image shows the same embryos under different illuminations. (**g**) Transfer of the embryos from the apple juice segment to the imaging slide. (**h**) Incubation with 50 µl of halocarbon oil added dropwise to the embryos. (**i**) Finished slide ready for

imaging. After incubation with halocarbon oil a larger 22x40 coverslip is overlaid and the short ends sealed with nail varnish.

Figure 2. Performing FRAP and data acquisition. (**a**) Cartoon representation of a late stage *Drosophila* embryo. The area representing the dorsolateral epidermis which is used for the FRAP experiment is highlighted by the square. (**b**) The cells of the epidermis of the stage 15 embryo have a distinct rectangular morphology: with long anterior-posterior (AP) and short dorsal-ventral (DV) cell borders. The regions of interest (ROI) which are to be bleached are shown (red circles), in this case two DV and one AP borders are indicated. The ROI are the same shape and diameter to maintain a consistent diffusion coefficient. A z-stack of six slices is positioned to bleach the signal in the ROI in the Z-axis (Time=-20 sec). (**c**) Signal in the ROI immediately after bleaching (Time=0 sec). Some signal is still visible in the ROI, an initial indicator that bleaching was not too strong. (**d**) The area and bleached ROI at the end of the experiment (total 15 minutes for E-cad in the embryonic epidermis). More signal is now evident in the ROI and the tissue has shifted position during the course of the experiment. Each of the z-stacks is projected for each time point giving a total number of 45 timepoints for this experiment (time = 900 sec). (**e**) The three measurements which are taken for each timepoint for analysis: the bleached ROI in which the signal recovery after bleaching is recorded (red); the control area (blue) to account for bleaching during acquisition; and the background signal (green). Scale bar = 10μm.

Figure 3. Plotting recovery curves. (**a-b**) Representation of the recovery of E-cad-GFP in the embryonic epidermis. (**a**) Recovery of the E-cad signal at the long (AP) cell borders. The signal recovers to approximately 50% of the fraction which was bleached. The signal which recovers corresponds to the protein which is exchanged at the time-scale of the experiment, therefore is termed the mobile fraction or the unstable fraction. The proportion of the bleached signal which does not recover, meaning the protein does not exchange at this time-scale, is called the immobile or stable

fraction. The line represents the non-linear fit curve and the individual points are means with the bars representing the SEM. (**b**) The same data but showing the individual traces for each of the replicates with the line of best fit for the non-linear analysis shown in red. This graph indicates the variability inherent in FRAP experiments and the necessity of having sufficient sample size to mitigate this effect and derive valid and accurate conclusions from any comparative analysis (n= 6 embryos, each embryo had two borders bleached and the average of these was used as an embryo average).
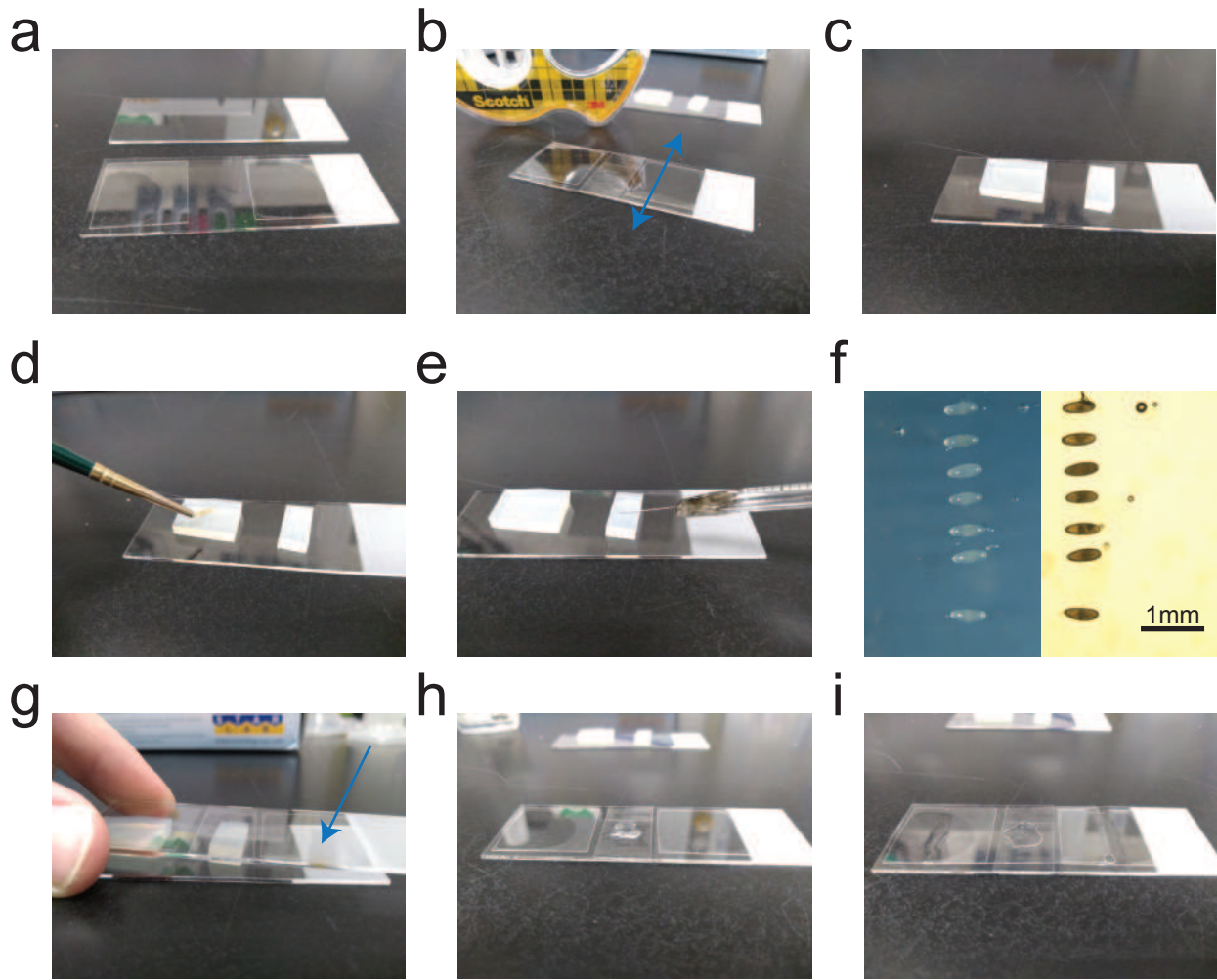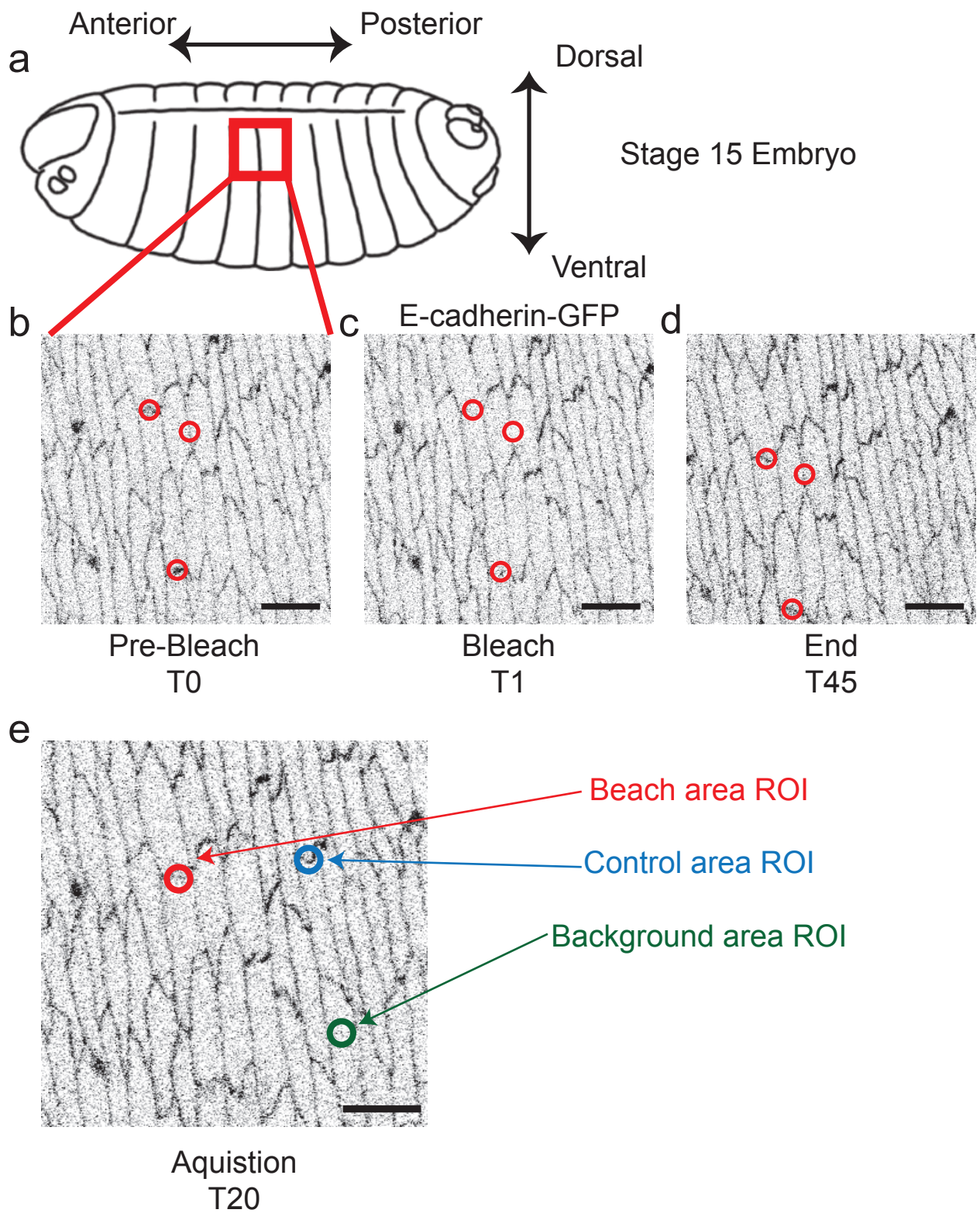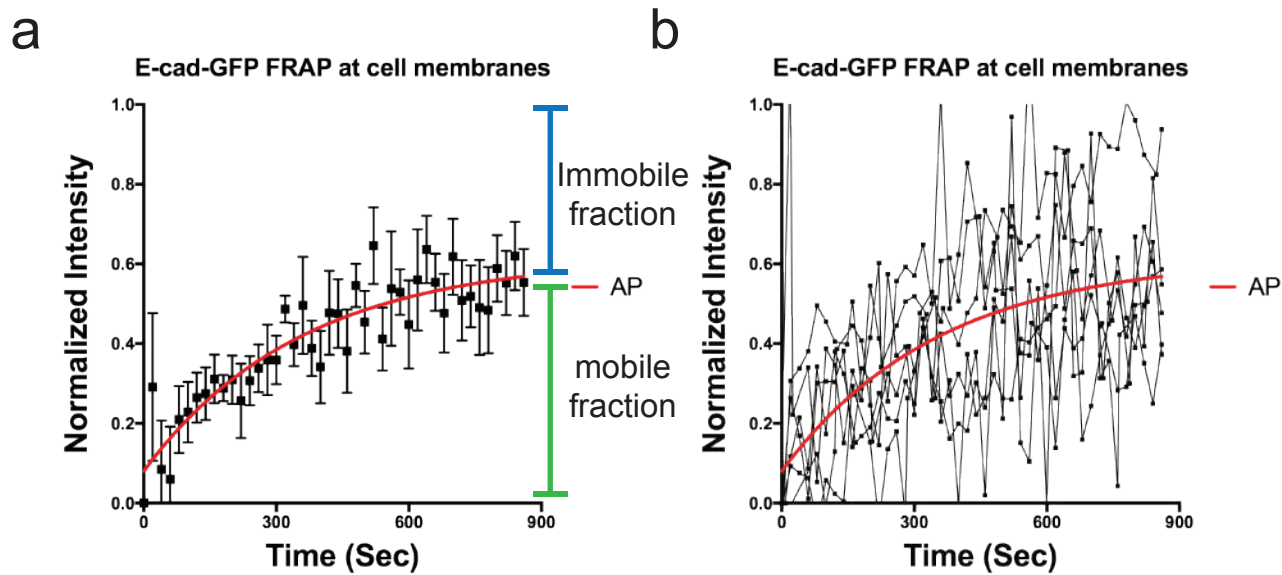
Fig. 1

a

Anterior ← → Posterior

Dorsal ↕ Ventral

Stage 15 Embryo

b Pre-Bleach T0

c E-cadherin-GFP — Bleach T1

d End T45

e Aquistion T20

Beach area ROI

Control area ROI

Background area ROI

Fig. 2

Fig. 3